

Quasi two-dimensional Fermi surface topography of the delafossite PdRhO₂

F. Arnold,¹ M. Naumann,^{1,2} S. Khim,¹ H. Rosner,¹ V. Sunko,^{1,3} F. Mazzola,³ P.D.C. King,³ A.P. Mackenzie,^{1,3,*} and E. Hassinger^{1,2,*}

¹Max Planck Institute for Chemical Physics of Solids, 01187 Dresden, Germany

²Physik-Department, Technische Universität München, 85748 Garching, Germany

³Scottish Universities Physics Alliance, School of Physics and Astronomy, University of St. Andrews, St. Andrews, Fife KY16 9SS, UK

(Dated: August 7, 2017)

We report on a combined study of the de Haas-van Alphen effect and angle resolved photoemission spectroscopy on single crystals of the metallic delafossite PdRhO₂ rounded off by *ab initio* band structure calculations. A high sensitivity torque magnetometry setup with SQUID readout and synchrotron-based photoemission with a light spot size of 50 μm enabled high resolution data to be obtained from samples as small as 150 × 100 × 20 (μm)³. The Fermi surface shape is nearly cylindrical with a rounded hexagonal cross section enclosing a Luttinger volume of 1.00(1) electrons per formula unit.

PACS numbers: 71.27.+a,71.18.+y,71.15.Mb

In recent years delafossite layered metallic oxides [1] have attracted considerable attention because of their extremely high electrical conductivity and the simplicity of their electronic structure [2]. The delafossite structure of general formula ABO₂ features alternating triangularly co-ordinated A metal layers separated by BO₂ layers in which B is a transition metal in a trigonally distorted octahedral co-ordination with oxygen [3]. The layer stacking sequence results in there being three formula units per hexagonal unit cell, with the space-group $R\bar{3}m$. Many delafossites are semiconducting or insulating, but those with A site metals Pd or Pt are highly anisotropic metals in which conductivity in the layers is hundreds of times larger than that perpendicular to them. Even at room temperature, the in-plane resistivities of non-magnetic PtCoO₂ and PdCoO₂ are just over 2 μΩcm [4, 5], lower than that of any elemental metal except Ag and Cu. Taking into account the factor of three lower carrier density in the delafossites, they have a room temperature mean free path at least a factor of two longer than even that of pure Ag. The resistivity falls rapidly with temperature, and resistive mean free paths of over 20 μm have been observed in PdCoO₂ [4].

The Fermi surface (FS) of the known delafossite metals is extremely simple. In non-magnetic PdCoO₂ and PtCoO₂, it is a single, weakly corrugated cylinder with nearly hexagonal cross-section [5–9]. In PdCrO₂, a similar cylinder is observed above 40 K, but at low temperatures very small gapping is detected, due to coupling between spin ordering in the CrO₂ layers and the states in the broad conduction band whose dominant character is Pd *4d/5s*-like [10–13]. Electron counting in PdCrO₂ highlights the role of correlations in the transition metal layer of the delafossites: the CrO₂ layer is Mott insulating [13].

The knowledge to date of the delafossite metals therefore points to an interesting and very unusual situation

in which there is a close interplay between an extremely broad conduction band with a Fermi velocity of order $8 \times 10^5 \text{ ms}^{-1}$ (close to the free electron value) and *3d* transition metal states for which correlations are known to be strong. The situation is made even richer by the fact that the weakly- and strongly-correlated states arise from different layers in the crystal structure. Delafossites are like a naturally-occurring example of the kind of heterostructures that many groups world-wide are trying to synthesize artificially, and a natural structural class on which to base future layer-by-layer synthesis.

The unique combination of properties highlighted above has already led to the observation of fascinating physics, notably the observation of huge c-axis magnetoresistance oscillations [14, 15], the unconventional Hall effect [16], and hydrodynamic electron flow [17], and it seems likely that new regimes of mesoscopic transport will be attainable via focused ion beam microstructuring of single crystals.

All of these phenomena are expected to be strongly sensitive to the details of the FS shape, i.e. the curvature of the in-plane hexagon, as well as the out-of-plane warping. To unlock the full potential of the delafossite oxides and to yield new physics, it is crucial to have access to slightly different FS topographies and different levels of correlation in the ABO₂ layers, while preserving the overall simplicity of the electronic structure. There is a pressing need, therefore, to have as many such metals available for precision study as possible. So far, the only monovalent delafossite metals for which single crystals exist are PdCoO₂, PdCrO₂ and PtCoO₂ in which the B-site cations are *3d* transition metals [18]. Based on preliminary studies on powders and polycrystalline thin films, as well as electronic structure calculations [19–21], PdRhO₂ is thought to be metallic and also to have a single conduction band. Hence this material offers the opportunity to study the effect of varying Pd-Pd overlap

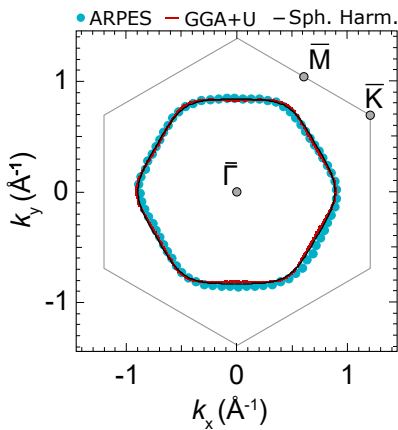


Figure 1. Planar Fermi surface topography of PdRhO₂ as determined by angle-resolved photo-emission spectroscopy (ARPES), density functional theory (DFT) calculations, and in-plane Fermi surface harmonics quoted later in Tab. I. DFT and surface harmonics data have been rescaled by -6% to fit the ARPES results.

integrals, as well as the effect of changing on-site correlation and spin-orbit coupling strengths by moving to a $4d$ B site transition metal.

Recently, we have succeeded in crystallizing PdRhO₂ [22]. Here, we report a comprehensive study of de Haas-van Alphen (dHvA) measurements on this new material, and combine the dHvA data with information from angle resolved photoemission spectroscopy (ARPES) to determine the FS with high precision. We also highlight the potential of PdRhO₂ to test and refine the accuracy of modern many-body electronic structure calculations.

Crystal growth and characterization of single crystals of PdRhO₂ is described in [22, 23]. De Haas-van Alphen oscillations of two PdRhO₂ crystals from the same growth batch were observed at temperatures between 100 mK and 4 K in magnetic fields up to 15 T. The respective sample sizes were approximately $200 \times 300 \times 50 (\mu\text{m})^3$ and $150 \times 100 \times 20 (\mu\text{m})^3$. Experiments were performed using an ultra-low noise SQUID torque magnetometer, installed on a MX400 Oxford Instruments dilution refrigerator with a 15/17 T superconducting magnet and 270° Swedish rotator with an angular accuracy of $\Delta\theta = \pm 0.2^\circ$. The magnetometer utilizes piezoresistive PRC400 micro-cantilevers and a two-stage dc-SQUID as highly sensitive read-out, offering an unprecedented torque resolution of $\Delta\tau = 2 \times 10^{-13}$ Nm at lowest temperatures [24, 25]. Data were taken at constant temperatures whilst the magnetic field was swept from 15 to 7.5 T at a rate of 30 mT/min.

ARPES was performed using the I05 beamline of Diamond Light Source, UK. Samples were cleaved in-situ at the measurement temperature of 13 K, and probed using linear horizontal polarisation light with a photon energy of 110 eV and spot size of $\approx 50 \mu\text{m}$. As well as the bulk FS extracted here, surface states indicative of a RhO₂-

termination were also observed in the experiment [26].

Relativistic density functional (DFT) electronic structure calculations including spin-orbit coupling were performed using the full-potential FPLO code [27–29], version fplo14.00-47 within the general gradient approximation (GGA). Coulomb repulsion in the Rh- $4d$ shell was simulated in a mean field way applying the GGA+ U approximation in the atomic-limit-flavor [22, 23].

The calculated and ARPES-measured FS of PdRhO₂ are compared in Fig. 1. The ARPES measurements yield a Luttinger count of 0.94(4) electrons per formula unit. Similar to ARPES measurements of other metallic delafossites [5, 10], this is slightly smaller than the half-filled band expected from electron counting, which is likely due to a small shift of the Fermi level arising from a polar surface charge. Nonetheless, apart from some small distortions related to details of the experiment [23], the measured FS is in good agreement with the projection of that calculated from density-functional theory on to the two-dimensional Brillouin zone, if they are scaled to the same total area. The calculations indicate a highly two-dimensional FS, entirely consistent with sharp spectral line widths observed in the ARPES which rule out significant k_z dispersion. These therefore show that the interplane dispersion in PdRhO₂ is extremely small; the de Haas-van Alphen effect is one of the few experimental probes capable of resolving the resulting k_z dependent features in the FS [30].

In Figure 2 we show background subtracted magnetic torque data for a selection of magnetic field angles θ with respect to the crystallographic c -axis within the ZFL-plane. Strong quantum oscillations are visible for all magnetic field angles (see Fig. 2a) and b)). The $1/\cos(\theta)$ angular dependence of the two quantum oscillation frequencies (dashed line in Fig. 2c) evidences the quasi-two-dimensional FS topography, while the beating of the envelope function is the first indication of out-of-plane dispersion. The lower and higher frequencies, labeled F_β and F_α , correspond to minimal and maximal extremal orbits respectively. These are also evident in the Fourier transforms of Fig. 2c), which were taken over a magnetic field interval from 7.5 to 15 T. For better accuracy the frequency splitting close to the Yamaji angles was derived from the beating envelopes.

For $B\parallel c$, the mean quantum oscillation frequency $\bar{F}_0 = (F_\alpha(0) + F_\beta(0))/2 = 26.25$ kT is equivalent to a FS cross section of $A = 2.505 \text{ \AA}^{-2}$. Considering the room-temperature lattice constants [22] this corresponds to 50.3% filling of the first Brillouin zone (4.9814 \AA^{-2}) and Luttinger count of 1.006(10), where the error estimate is dominated by the likely effects of thermal contraction. Thus, in agreement with *ab-initio* band structure calculations, the electronic structure of PdRhO₂ is described by a single half-filled band with 1.00 charge carriers per formula unit.

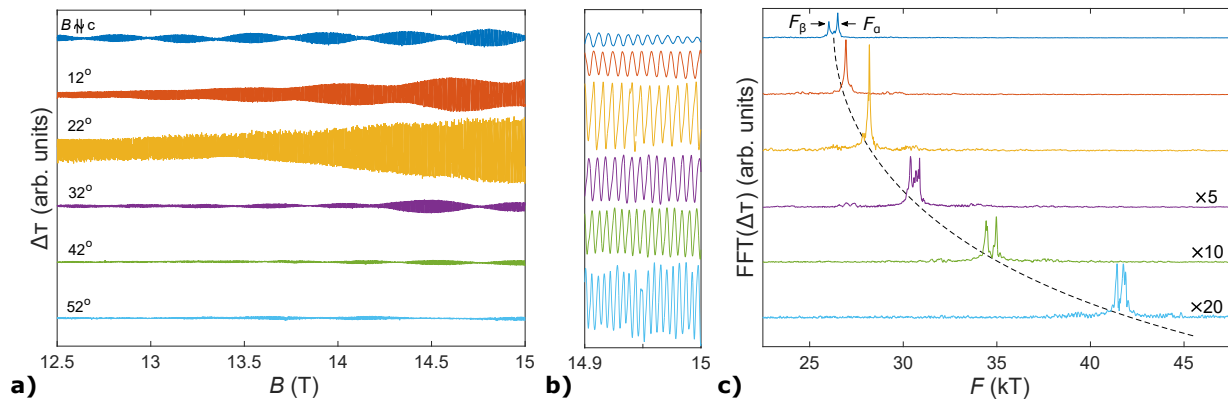


Figure 2. Magnetic torque de Haas-van Alphen signal of PdRhO₂ at $T \approx 100$ mK. **a)** shows the magnetic field dependence of the de Haas-van Alphen oscillations for a selection of magnetic field angles within the ZFL-plane. The data were background subtracted by a 2nd-order polynomial. A zoom of the high field oscillations is shown in **b)**. **c)** displays the Fourier transforms corresponding to the oscillations shown in **a)**. Data have been multiplied and offset for clarity. The dashed line shows the $1/\cos(\theta)$ -angular dependence of the mean quantum oscillation frequency \bar{F} for a 2D Fermi surface.

The effective cyclotron mass, Dingle temperature and mean free path were determined for fields close to the c -axis. Details of the analysis are given in [23]. The key results are the masses $m_\alpha = 1.43(5) m_0$ and $m_\beta = 1.63(5) m_0$ and the mean free path is 225(30) nm.

In order to analyze the FS topography further, we now turn to the angular dependence of the observed frequency splitting. The quantum oscillation frequencies for magnetic fields within the crystallographic ZFK and ZFL-planes corrected by $\cos(\theta)$ are shown in Fig. 3. Only the frequency splitting around the mean frequency \bar{F} is shown, as the angular inaccuracy of our rotator leads to sizable frequency offsets especially at larger angles. For the raw data and detailed analysis of the angular uncertainty see [23].

The FS warping, i.e. azimuthal and height dependence of k_F , can be parametrised in cylindrical harmonics:

$$k_F = \sum_{\mu, \nu \geq 0} k_{\mu, \nu} \cos(\nu \kappa) \cos(\mu \phi), \quad (1)$$

where $\kappa = c^* k_z$ is the reduced z -coordinate and ϕ the azimuthal angle [31]. Note that $c^* = 6.034 \text{ \AA}$ is the interlayer spacing, which is a third of the c -axis lattice constant. Due to the hexagonal lattice symmetry and $R\bar{3}m(D_{3d}^5)$ space group, $k_{\mu, \nu}$ are limited to $(\mu, \nu) \in \{(0, 0); (0, 1); (0, 2); (0, 3); (3, 1); (6, 0); (12, 0)\}$ and higher order terms. By fitting to the frequencies shown in Fig. 3, as described in detail in [23], we are able to determine $k_{0,0}$ and all relevant $k_{\mu\nu}$ with $\nu \geq 1$. The in-plane parameters $k_{6,0}$ and $k_{12,0}$ were obtained from the FS shape of Fig. 1 [23]. The respective parameters and FS topology are summarized in Tab. I.

Here, $k_{0,0}$ is uniquely determined by the mean quantum oscillation frequency $k_{0,0} = \sqrt{2e\bar{F}_0/\hbar}$ for $B||c$, whilst $k_{0,1}$ is mostly responsible for the frequency splitting around the c -axis. $k_{3,1}$ is determined by the asym-

metry between positive and negative field angles within the ZFL-plane (Fig. 3b). Note that we had to allow for a $\approx 2^\circ$ azimuthal misalignment of ZFK rotation plane to account for the observed asymmetry between positive and negative polar angles in Fig. 3a. Otherwise (for perfect alignment) the quantum oscillation frequencies within the ZFK plane are independent of $k_{3,1}$ and symmetric about $\theta = 0$. The parameter $k_{0,2}$ results in an asymmetry of the angular dependence of the upper versus the lower frequency branch. By a comparison of the raw data in Fig. 7 of the Supplemental Online Material [23] with the simulation, we estimate that $k_{0,2} < 0.0002 \text{ \AA}^{-1}$.

Knowledge of the warping parameters of PdRhO₂ and a comparison with those previously deduced for its sister compound PdCoO₂ [4] yields considerable insight into interplane hopping and coherence in the metallic delafossites. In both materials the dominant interplane terms are $k_{0,1}$, qualitatively corresponding to direct Pd-Pd hopping along the c -axis, and $k_{3,1}$, which results from hopping via the Co or Rh layers. In going from Co to Rh, several effects are expected to compete. Rh is larger, with more extended $4d$ orbitals, so its presence increases the in-plane a and interplane c lattice parameters, by approximately 7% and 2% respectively. This lattice expansion would be expected to lead to less effective c -axis Pd-Pd hopping, consistent with the observation that $k_{0,1}$ is a factor of 2.7 smaller in PdRhO₂ than in PdCoO₂. For hopping via the Co/Rh layer the situation is more subtle. If correlations in that layer are ignored, an LDA calculation predicts a much larger $k_{3,1}$ term in PdCoO₂ than is actually observed. However, if some account is taken of that correlation by assuming a realistic on-site repulsion energy U of several eV [4, 23], the hybridization with the conduction band is strongly suppressed, reducing the calculated value to close to the experimental one of $k_{3,1} = 0.001 \text{ \AA}^{-1}$. Qualitatively, the lattice parame-

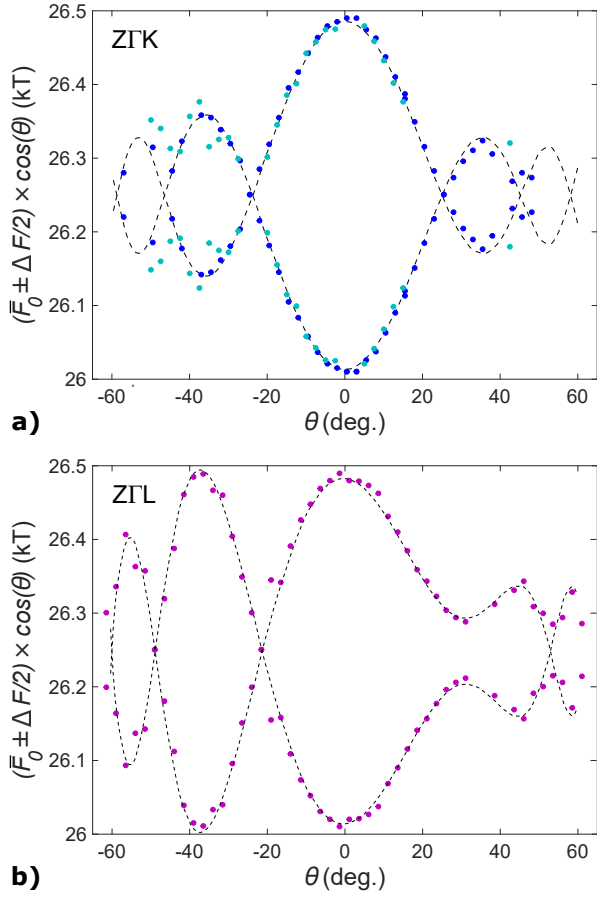


Figure 3. The graph shows the angular dependence of the quantum oscillation frequencies for magnetic field angles within the crystallographic ZΓK-plane (a) and ZΓL-plane (b). Dark blue and violet symbols are data points taken on the same PdRhO₂ single crystal, whereas light blue symbols originate from a second sample from the same growth batch. Black dashed lines correspond to the cylindrical harmonic expansion of best fit. The associated harmonic parameters can be found in Tab. I.

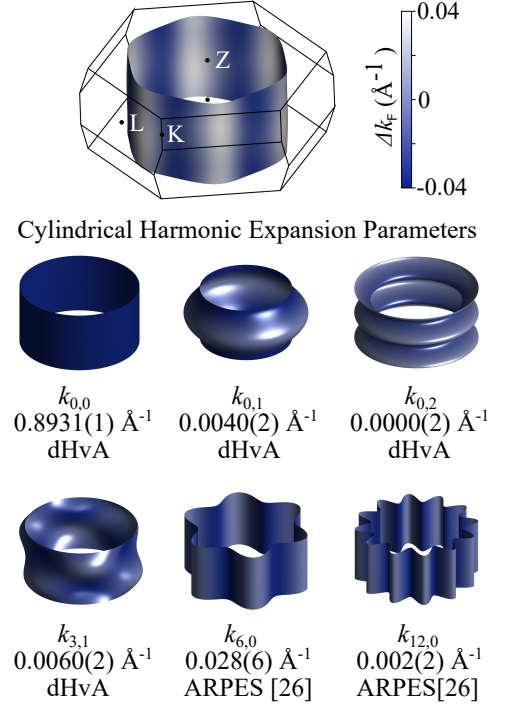
ter expansion caused by moving from Co to Rh, which naively would be expected to reduce $k_{3,1}$, is more than offset by the reduction in U for the $4d$ states of Rh and an increase in Pd-Rh overlap. The result is a slightly larger value of $k_{3,1} = 0.006 \text{ \AA}^{-1}$.

Overall, the FS of PdRhO₂ is extremely anisotropic, and the most two-dimensional of any metallic delafossite. Under the assumption of a single scattering time τ , the $k_{\mu,\nu}$ harmonics can be used to estimate the resistive anisotropy. For a single band metallic delafossite with an assumed circular FS (the hexagonal cross-section of Fig. 1 only alters this estimate by a few per cent) the relevant expression is

$$\frac{\rho_{ab}}{\rho_c} = \frac{c^{*2}}{2} \sum_{\mu,\nu} \nu^2 k_{\mu,\nu}^2 (1 + \delta_{\mu 0}) \quad (2)$$

where δ is the Kronecker delta function [30, 32]. Since

Table I. Experimentally determined cylindrical harmonic expansion parameters of PdRhO₂:



$k_{0,1}$ contributes more strongly to this sum than $k_{3,1}$, PdRhO₂ is predicted to have a larger anisotropy (≈ 800) than PdCoO₂. Preliminary transport data [22] are consistent with this prediction, though a more careful transport study with a range of sample sizes is desirable. The larger size of Rh also affects the in-plane Pd-Pd overlaps and reduces $k_{6,0}$, $k_{12,0}$ and the Fermi velocity v_F . Using $k_{0,0}$ and the measured masses leads to a Brillouin zone averaged Fermi velocity $\bar{v}_F = \hbar k_{0,0}/m^* = 6.8 \times 10^5 \text{ ms}^{-1}$. This is smaller than that of PdCoO₂ by approximately 10%, consistent with the a lattice parameter being 7% larger in PdRhO₂.

Although it is possible to qualitatively account for the trends of the warping harmonics and Fermi velocity on going from PdCoO₂ to PdRhO₂, the resolution of the data that we have presented provides a considerable opportunity to refine the quality of electronic structure calculations. Despite the lower correlation energies for $4d$ Rh and Pd than for $3d$ transition metals, correlation still plays an important role in determining the details of the observed FS, and in tuning the degree of interlayer hopping. Knowing the experimental warpings at 0.1% resolution presents a considerable challenge to "ab initio plus correlation" theoretical approaches. It will be intriguing to see if any are capable of accounting for the values that we report for $k_{6,0}$, $k_{12,0}$, $k_{0,1}$, $k_{0,2}$, $k_{3,1}$ and v_F . Although this seems a difficult task, PdRhO₂ will be an ideal material on which to benchmark the progress of the field. Preliminary attempts to add a single U on the Rh site

were not successful in matching all the parameters simultaneously; refinement at the level of individual Wannier functions is likely to be necessary.

A further property of note is the extremely high overall anisotropy of the measured FS. If sufficiently high anisotropies can be obtained in very clean materials like the metallic delafossites, it is possible that at high magnetic fields a limit could be reached in which all electrons are restricted to a single Landau level of very high index. Hence the physics of singly occupied Landau levels, long thought to be restricted to low density electron gases, might be observable at full metallic electron densities. Although the total bandwidth along k_z in as-grown PdRhO₂ is very small, it is still 40 meV, implying that a field of nearly 500 T would be required to reach this limit. However, this observation provides motivation to try to produce a still more anisotropic material, perhaps using uniaxial pressure in PdRhO₂ or by growing crystals of the next compound in the series, PdIrO₂. This latter material is also of considerable interest as a candidate triangular lattice superconductor.

In summary, we have successfully established the Fermi surface topography of the metallic delafossite PdRhO₂, using a combination of angle-resolved photoemission spectroscopy and high resolution torque magnetometry studies of the de Haas-van Alphen effect. Our results establish it as a benchmark material for the study of high purity quasi-two dimensional metals, and for the development of high precision electronic structure calculations.

ACKNOWLEDGMENTS

The authors would like to thank the Diamond Light Source for access to Beamline I05 via Proposal No. SI14927 as well as L. Bawden, T.K. Kim, and M. Hoesch for their technical support. In addition we would like to acknowledge the financial support from the European Research Council (through the QUESTDO project), the Engineering and Physical Sciences Research Council UK (Grant No. EP/I031014/1 and EP/L015110/1), the Royal Society and the Max-Planck Society.

* correspondence should be addressed to mackenzie@cpfs.mpg.de and elena.hassinger@cpfs.mpg.de

- [1] R. D. Shannon, D. B. Rogers, and C. T. Prewitt, *Inorg. Chem.* **10**, 713 (1971).
- [2] A. P. Mackenzie, *Rep. Prog. Phys.* **80**, 032501 (2017).
- [3] C. T. Prewitt, R. D. Shannon, and D. B. Rogers, *Inorg. Chem.* **10**, 719 (1971).
- [4] C. W. Hicks, A. S. Gibbs, A. P. Mackenzie, H. Takatsu, Y. Maeno, and E. A. Yelland, *Phys. Rev. Lett.* **109**, 116401 (2012).
- [5] P. Kushwaha, V. Sunko, P. J. W. Moll, L. Bawden, J. M. Riley, N. Nandi, H. Rosner, M. P. Schmidt, F. Arnold, E. Hassinger, T. K. Kim, M. Hoesch, A. P. Mackenzie, and P. D. C. King, *Sci. Adv.* **1**, e1500692 (2015).
- [6] V. Eyert, R. Frésard, and A. Maignan, *Chem. Mater.* **20**, 2370 (2008).
- [7] K. Kim, H. C. Choi, and B. I. Min, *Phys. Rev. B* **80**, 035116 (2009).
- [8] K. P. Ong, D. J. Singh, and P. Wu, *Phys. Rev. Lett.* **104**, 176601 (2010).
- [9] H.-J. Noh, J. Jeong, J. Jeong, E.-J. Cho, S. B. Kim, K. Kim, B. I. Min, and H.-D. Kim, *Phys. Rev. Lett.* **102**, 256404 (2009).
- [10] J. A. Sobota, K. Kim, H. Takatsu, M. Hashimoto, S.-K. Mo, Z. Hussain, T. Oguchi, T. Shishidou, Y. Maeno, B. I. Min, and Z.-X. Shen, *Phys. Rev. B* **88**, 125109 (2013).
- [11] J. M. Ok, Y. J. Jo, K. Kim, T. Shishidou, E. S. Choi, H.-J. Noh, T. Oguchi, B. I. Min, and J. S. Kim, *Phys. Rev. Lett.* **111**, 176405 (2013).
- [12] H.-J. Noh, J. Jeong, B. Chang, D. Jeong, H. S. Moon, E.-J. Cho, J. M. Ok, J. S. Kim, K. Kim, B. I. Min, H.-K. Lee, J.-Y. Kim, B.-G. Park, H.-D. Kim, and S. Lee, *Sci. Rep.* **4**, 3680 (2014).
- [13] C. W. Hicks, A. S. Gibbs, L. Zhao, P. Kushwaha, H. Borrmann, A. P. Mackenzie, H. Takatsu, S. Yonezawa, Y. Maeno, and E. A. Yelland, *Phys. Rev. B* **92**, 014425 (2015).
- [14] H. Takatsu, J. J. Ishikawa, S. Yonezawa, H. Yoshino, T. Shishidou, T. Oguchi, K. Murata, and Y. Maeno, *Phys. Rev. Lett.* **111**, 056601 (2013).
- [15] N. Kikugawa, P. Goswami, A. Kiswandhi, E. S. Choi, D. Graf, R. E. Baumbach, J. S. Brooks, K. Sugii, Y. Iida, M. Nishio, S. Uji, T. Terashima, P. M. C. Rourke, N. E. Hussey, H. Takatsu, S. Yonezawa, Y. Maeno, and L. Balicas, *Nature Commun.* **7**, 10903 (2016).
- [16] H. Takatsu, S. Yonezawa, S. Fujimoto, and Y. Maeno, *Phys. Rev. Lett.* **105**, 137201 (2010).
- [17] P. J. W. Moll, P. Kushwaha, N. Nandi, B. Schmidt, and A. P. Mackenzie, *Science* **351**, 1061 (2016).
- [18] AgNiO₂ is also metallic, but as the result of charge order in the B site Ni layer, is distinct from the monovalent metals discussed here. See A. I. Coldea *et al.* *ArXiv Preprint* <http://arxiv.org/abs/0908.4169> (2009).
- [19] R. J. Baird, G. W. Graham, and W. H. Weber, *Oxid. Met.* **29**, 435 (1988).
- [20] P. F. Carcia, R. D. Shannon, P. E. Bierstedt, and R. B. Flippen, *J. Electrochem. Soc.* **127**, 1974 (1980).
- [21] K. Kim, J. Kim, and B. I. Min, *J. Phys. Soc. Jpn.* **83**, 124708 (2014).
- [22] P. Kushwaha, H. Borrmann, S. Khim, H. Rosner, P. J. W. Moll, D. A. Sokolov, V. Sunko, Y. Grin, and A. P. Mackenzie, *arXiv:1706.07614 [cond-mat]*.
- [23] Supplemental Material at [http:// ...](http://...)
- [24] F. Arnold, M. Naumann, T. Lühmann, A. P. Mackenzie, and E. Hassinger, (2017), *arXiv:1706.08350 [physics.ins-det]*.
- [25] C. Rossel, P. Bauer, D. Zech, J. Hofer, M. Willemin, and H. Keller, *J. Appl. Phys.* **79**, 8166 (1996).
- [26] V. Sunko, H. Rosner, A. P. Mackenzie, and P. D. C. King, *et al.*, to be published.
- [27] K. Koepernik and H. Eschrig, *Phys. Rev. B* **59**, 1743 (1999).
- [28] I. Opahle, K. Koepernik, and H. Eschrig, *Phys. Rev. B* **60**, 14035 (1999).

- [29] www.fpl0.de.
- [30] C. Bergemann, A. P. Mackenzie, S. R. Julian, D. Foresythe, and E. Ohmichi, *Adv. Phys.* **52**, 639 (2003).
- [31] C. Bergemann, S. R. Julian, A. P. Mackenzie, S. NishiZaki, and Y. Maeno, *Phys. Rev. Lett.* **84**, 2662 (2000).
- [32] N. W. Ashcroft, and D. N. Mermin, *Solid State Physics* (Philadelphia: Saunders College Publishing, 1976)